Gait Simulation for Asymmetric Gait

Zhongxiang Chen[a], Tomislav Bacek[b], Mingrui Sun[b], Hengchang Liu[b], Denny Oetomo[b], Ying Tan[b], Dana Kulić[a]
[a]Monash University [b]The University of Melbourne, Australia
zhongxiang.chen@monash.edu

Abstract

Predictive gait simulation aims to predict the motion and loading characteristics of gait, given an individualised model. It can be used to identify the underlying causes of asymmetric gait, and predict how a patient will respond to intervention, thus providing personalised assistance to patients. However, most studies focus on healthy gait and assume that the gait is symmetric between the right and left side. This assumption reduces the computational cost significantly but may not be appropriate for patient gait. In this paper, we relax the symmetry assumption and predict the entire stride directly. Next, a simplified skeletal model was developed to reduce the computational demand. The simulated results were compared to experimental data of asymmetric gait, showing that the proposed method could generate joint angle and ground reaction forces similar to constrained walking, with limitations due to the simplified model and cost function.

1 Introduction

Gait simulation is studied by many researchers in the fields of rehabilitation, human robot interaction, skill acquisition and athletic training [Kulić *et al.*, 2016]. Improved understanding of human gait can provide personalised assistance to patients. One path towards these insights is to generate gait using physics-based predictive simulations.

The assumption that natural structures and processes such as locomotion are optimal is one of the fundamentals of biomechanics [Alexander, 1984; Alexander, 1996]. Following the assumption, dynamics tasks such as walking and running can be simulated and analysed as optimal control problems [Chow and Jacobson, 1971; Felis *et al.*, 2015; Felis and Mombaur, 2016]. The selection of dynamic models is very important when generating gait simulations. Simple conceptual models such as the inverted pendulum model [Kajita *et al.*, 1992; Kudoh and Komura, 2003] can be used to solve the optimisation problem efficiently, but they do not provide enough details to analyse gait at the joint level.

On the other hand, complex musculoskeletal models can replicate human structure accurately, but are computationally expensive to solve. A recent study has shown that the computational cost of the optimisation could be reduced by using direct collocation, implicit differential equations and algorithmic differentiation [Falisse *et al.*, 2019]. Although the simulated gait was assumed to be symmetric to reduce the scale of the problem, the average time taken to find the optimal solutions was still more than half an hour.

In this work we present our approach to simulate asymmetric gaits by formulating walking as an optimal control problem with skeletal models. The accuracy of the simulated results were compared with experimental data collected from a healthy participant. The main contributions of our work are the following:

- Reformulated the approach of [Falisse *et al.*, 2019] to allow simulation of asymmetric gait.
- A simplified skeletal model is investigated to reduce the computational cost of the optimisation problem.
- Symmetric and asymmetric gait generated by the proposed approach is compared with preliminary experimental data.

The remainder of this paper is organised as follows. In Section 2, related work on predictive gait simulation and dynamic models is briefly reviewed. Section 3 overviews the problem formulation, model selection and assumption relaxation approach. Section 4 summarises the experimental setup and data collection. Section 5, analyses the simulated results and compares the predictions with experimental results. Finally, Section 6 concludes the paper and discusses next steps.

2 Related Work

Optimal control has been widely used for simulating and analysing human walking and running. For example, human data of reaching movements [Flash and Hogan, 1985], postural balance [Kuo, 1995] and gait [Felis *et al.*, 2015; Felis and Mombaur, 2016] have all been shown to be well predicted by optimisation. To solve the optimal control problem, the system dynamic model, objective function and constraints must be specified, and a solution method chosen.

2.1 Dynamic models

There is a large number of dynamic models used for the study of human walking, varying in kinematic complexity and dynamic formulation.

The 2D inverted pendulum model (IPM) is the simplest model which contains a single mass at the hip and two weightless legs [Kajita *et al.*, 1992]. It assumes that both hip joints only move in the sagittal plane and zero ankle torque around the contact points with the ground. A closed-form solution is easily obtained due to the simplicity of the system dynamics and these assumptions, enabling gait generation for a biped robot in real time. The model was extended to a 3D inverted pendulum model which allows the movement of mass in the frontal plane [Kajita *et al.*, 2001]; angular-momentum-inducing inverted pendulum model which takes consideration of angular momentum around the center of gravity [Kudoh and Komura, 2003]; and a gravity-compensated inverted pendulum model which added a mass for the swing leg and produced more stable walking motion than IPM [Park and Kim, 1998]. While inverted pendulum models have been widely used in gait analysis and bipedal robot design and control, they are not suitable for the study of motion and forces at individual joint-level.

On the other spectrum of kinematic complexity is a full-body biomechanics model which aims to replicate the anatomical structure of the human body accurately. For example, a 37 degree of freedom (DOF) model was utilised for predicting muscle forces and joint moments in walking and running [Rajagopal *et al.*, 2016]. A 55 DOF model was created for predictions of various activities including walking, running, and jumping [Chung *et al.*, 2015; Bataineh *et al.*, 2016]. These models enable gait analyses and gaining insight into normal and abnormal human walking at the joint level, which could not be achieved with the simple models. However, getting closed-form solutions of these complex models is difficult, and numerical approaches are usually required. Biomechanics models can be further classified into skeletal(SK), musculoskeletal(MSK), and neuromusculoskeletal(NMSK) models based on the components included in the dynamics formulation[Ezati *et al.*, 2019]. The SK models only contain skeletal motion dynamics, which describes the relationship between joint torques, external forces and moments, and joint angles/velocities. The MSK models additionally have the musculoskeletal geometry and muscle contraction dynamics; while the NMSK models further expend on MSK models with muscle activation dynamics which output muscle activation given neural commands.

2.2 Methods for solving the optimal control problem

There are two approaches for solving the optimal control problem, namely the direct and indirect methods. The former method usually has the system dynamics formulated explicitly and the continuous input controls are treated as unknowns, which transforms the problem into a two-point boundary value problem (BVP)[Channon *et al.*, 1992; Saidouni and Bessonnet, 2003]. The later method discretises the states and controls by an appropriate function approximation and formulates the system dynamics implicitly, which transforms the problem to a nonlinear programming (NLP) problem[Hull, 1997; Anderson and Pandy, 2001]. When solving for human motions with a large number of degrees of freedom and stiff system dynamics, the indirect method is easier to solve and frequently used in the literature[Xiang *et al.*, 2010; Meyer *et al.*, 2016; Lin and Pandy, 2017].

The framework proposed in [Falisse *et al.*, 2019] aims to reduce the computational cost of physics-based predictive simulation. Gait simulations were formulated as optimal control problems based on a set of multi-objective performance criteria in MATLAB (The Mathworks Inc., USA) using CasADi [Andersson *et al.*, 2019]. A 29 DoF MSK model was adapted from [Hamner *et al.*, 2010; Delp *et al.*, 2007] with additional passive stiffness and damping in the joints. The dynamics of the model was defined as implicit constraints and the optimisation problem is transformed into a sparse NLP problem solved by IPOPT [Wächter and Biegler, 2006]. A custom version of OpenSim and Simbody[Sherman *et al.*, 2011] was developed to enable the application of algorithmic differentiation to improve computational efficiency. The framework was able to generate healthy human-like gait simulations in an average of 36 min of computational time with symmetry assumption. A sensitivity analysis was conducted to support the nominal cost function they have identified by manually tuning the cost terms and their associated parameters. The gait patterns generated were compared with experimental data of healthy symmetric gait. Simulation results for novel hypotheses such as weak hip actuators, weak plantarflexors and walk-run transition were also discussed. However, symmetry assumption was applied in all these cases to minimise the scale of the problem and computational cost. The paper

briefly discusses extensions to asymmetric pathological gait but detailed implementation was not provided.

3 Proposed approach

The central neural system of human are known to behave like an optimal controller when generating gait [Todorov, 2004]. The proposed approach formulates gait simulation as an optimal control problem which is governed by a cost function which describes the objectives of performance criterion. Implicit formulation of dynamics and algorithmic differentiation were utilised to solve the problem efficiently. In addition, simplifying the dynamic model could result in rapid convergence of the solver.

3.1 Optimal control problem definition

A finite-horizon discrete optimal control problem can be described by the dynamic system, the cost function and any constraints. Given a dynamic system of the form:

$$\boldsymbol{x}_{k+1} = \boldsymbol{f}(\boldsymbol{x}_k, \boldsymbol{u}_k), k \in [0, T-1], \tag{1}$$

where $\boldsymbol{x}_k \in \mathbb{R}^m$ and $\boldsymbol{u}_k \in \mathbb{R}^n$ are the states and control input at time k, and $\boldsymbol{f}$ is the state transition equation which models the system dynamics. The cost function is defined as:

$$J = \sum_{k=0}^{T-1} L_k(\boldsymbol{x}_k, \boldsymbol{u}_k) + L_T(x_T), \tag{2}$$

where J is the total cost, L_k is the running cost at each time step and L_T is the terminal cost.

In addition, there may be equality or inequality constraints on the state and controls:

$$\boldsymbol{h}(\boldsymbol{x}, \boldsymbol{u}) = 0, \tag{3}$$

$$\boldsymbol{g}(\boldsymbol{x}, \boldsymbol{u}) <= 0, \tag{4}$$

where $\boldsymbol{h}$ describes the equality and $\boldsymbol{g}$ describes the inequality constraints.

The objective is to find the optimal state and control trajectory $[\boldsymbol{x}^*, \boldsymbol{u}^*]$ that minimises J.

L_k and L_T are commonly assumed to be a linear combination of relevant features with corresponding feature weights in optimal control problems [Lin *et al.*, 2021; De Groote *et al.*, 2016], thus, transforming the cost function into

$$J = \sum_{k=0}^{T} \boldsymbol{\omega}\boldsymbol{\phi}(\boldsymbol{x}_k, \boldsymbol{u}_k), \tag{5}$$

where $\boldsymbol{\phi}$: $\mathbb{R}^m \times \mathbb{R}^n \rightarrow \mathbb{R}^s$ is called the relevant feature vector with the i_{th} entry $\boldsymbol{\phi}_i$ representing one relevant feature for the running cost, and $\boldsymbol{\omega} \in \mathbb{R}^s$ is called the weight vector, with the i_{th} entry $\boldsymbol{\omega}_i$ called the feature weight corresponding to $\boldsymbol{\phi}_i$. The optimal solution to the problem is obtained when total cost is minimized, denoted by J^*.

3.2 Human Body Modelling

We start with the 29 DoF MSK model introduced by [Falisse *et al.*, 2019]. This model contains 29 Degrees of Freedom: 6 DoF at the pelvis; 3 DoF at the hip, shoulder and lumbar joints; 2 DoF at the ankle joints; 1 DoF at the knee and elbow joints. The model has 92 muscles, 8 muscles actuate across the lumbar joint while the rest drive the lower body joints. All the arm joints are driven with torque actuators. Following our intention to minimise the model complexity and computational cost, the model is simplified to a 16 DoF SK model. The pelvis is free to move in all degrees of freedom, hip and knee joints remain the same as the 29 DoF MSK model, while the ankle joint is restricted to move in the sagittal plane only. The mass of the upper body including torso are lumped with the pelvis, the effect on model's center of mass was not investigated due to time constraints. All muscles of the model are removed and actuation of joints is modified to be torque-driven. Both models are shown in Figure 1 below.

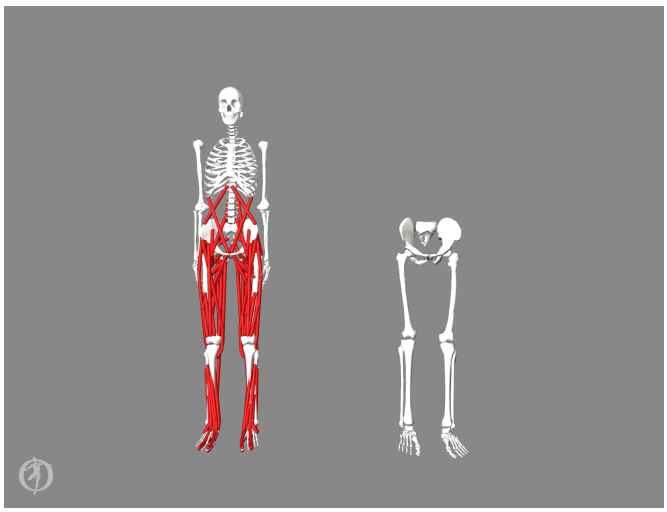

Figure 1: Biomechanical models used for gait simulation. The musculoskeletal model on the left has 29 DoF [Falisse *et al.*, 2019], and the skeletal model on the right has 16 DoF. Models are visualised in OpenSim.

3.3 Solution Approach

As reviewed in section 2.2, the indirect method is computationally efficient comparing to the direct methods. Therefore, the framework introduced by [Falisse *et al.*, 2019] was adapted to predict asymmetric gaits.

Implicit formulation of dynamics

The implicit formulation of the system dynamics of the 29 DoF MSK model was left unchanged as presented in the supplementary material of [Falisse *et al.*, 2019].

All the system dynamics are modelled directly in MATLAB apart from the skeletal motion dynamics which was implemented via the custom version of OpenSim and Simbody. The skeletal dynamics of the simplified SK model was implemented with these custom libraries, as discussed below.

In the forward dynamics approaches, the human body is commonly treated as a multi-body system and the skeletal dynamics can be described as:

$$\boldsymbol{M}(\boldsymbol{q})\ddot{\boldsymbol{q}} + \boldsymbol{C}(\boldsymbol{q}, \dot{\boldsymbol{q}})\dot{\boldsymbol{q}} + \boldsymbol{G}(\boldsymbol{q}) = \boldsymbol{S}^T\boldsymbol{\tau} + \boldsymbol{K}_c(\boldsymbol{q})^T\boldsymbol{F}_c \quad (6)$$

where $\boldsymbol{q}$, $\dot{\boldsymbol{q}}$ and $\ddot{\boldsymbol{q}}$ are the vectors of generalized joint coordinates, velocities and accelerations respectively, including both the inter-segment joints and the 6DoF floating base joint, $\boldsymbol{M}$ is the joint-space inertia matrix, $\boldsymbol{C}$ is the Coriolis and centripetal coupling matrix, $\boldsymbol{G}$ is the gravity terms, $\boldsymbol{S}$ is the Selection matrix selecting the actuated joints, $\boldsymbol{\tau}$ are the joint torques, $\boldsymbol{K}_c$ is the Contact Jacobian matrix, and $\boldsymbol{F}c$ are the external forces (e.g., the contact forces between foot and ground).

The implicit skeletal motion dynamics are described by the following equations:

$$\frac{d\boldsymbol{q}}{dt} = \boldsymbol{v}, \quad (7)$$

$$\frac{d\boldsymbol{v}}{dt} = \boldsymbol{u}_{dv}, \quad (8)$$

$$\boldsymbol{T} = \boldsymbol{f}_s(\boldsymbol{q}, \boldsymbol{v}, \boldsymbol{u}_{dv}), \quad (9)$$

where $\boldsymbol{T}$ are the net joint torques, $\boldsymbol{q}, \boldsymbol{v}, \boldsymbol{u}_{dv}$ are the joint coordinates, velocities and accelerations respectively which are equivalent to $\boldsymbol{q}$, $\dot{\boldsymbol{q}}$ and $\ddot{\boldsymbol{q}}$ in Equation 6. $\boldsymbol{f}_s(\cdot)$ in Equation 9 encapsulates the skeletal motion dynamics described by Equation 6. Note that $\boldsymbol{f}_s(\cdot)$ does not take $\boldsymbol{F}_c$ as an input because the contact forces are modelled within Simbody environment. The external forces will be calculated based on the joint kinematics and the interactions of the model with the environment prior to the computation of joint torques.

The actuation dynamics of the torque actuators in the skeletal model was implemented explicitly as the arm actuators in [Falisse *et al.*, 2019]:

$$\frac{d\boldsymbol{a}_{legs}}{dt} = \frac{\boldsymbol{e}_{legs} - \boldsymbol{a}_{legs}}{\tau}, \quad (10)$$

where $\tau = 35$ ms is a time constant. The state and control variables for each model are summarised in Table 1 given the implicit formulation of model dynamics.

The optimization variables and their corresponding dynamic constraints were scaled to the range of [-1, 1] using the same procedures described in [Falisse *et al.*, 2019]. The activations and excitations (a_{legs}, e_{legs}) of actuator-driven arm joints in the MSK model were scaled by a constant. For the simplified SK model, smoothed step functions of the scaling factors were implemented for a_{legs} and e_{legs} to retain the anatomical differences in the muscle distributions across the joints [Grimmer and Seyfarth, 2014; Bazett-Jones *et al.*, 2017; Moraux *et al.*, 2013].

Constraints

The following equality constraints are important for generating the walking motion using the proposed framework in [Falisse *et al.*, 2019], but were not explicitly discussed.

Firstly, since no external disturbances were applied when the human is walking voluntarily, therefore T_{pelvis} should be equal to null throughout the optimisation.

Secondly, to promote forward movement of the model the following equality constraints should be satisfied:

$$q_{pelvis,tx}(t_0) = 0, \quad (11)$$

$$q_{pelvis,tx}(t_h) = t_h v_{target}, \quad (12)$$

where $q_{pelvis,tx}$ is the translation of pelvis in forward direction, t_0 is the start of simulation which equals 0, t_h is the half gait cycle duration, and v_{target} is target speed of the simulated gait.

Lastly, the following equality constraints need to be satisfied assuming the gait is periodic and symmetric:

$$\boldsymbol{X}_{inverse}(t_0) = \overline{\boldsymbol{X}}_{inverse}(t_h), \quad (13)$$

$$\boldsymbol{X}_{oppose}(t_0) = -\boldsymbol{X}_{oppose}(t_h), \quad (14)$$

where $\boldsymbol{X}_{inverse}$ and $\boldsymbol{X}_{oppose}$ contains all state variables except $q_{pelvis,tx}$. $\boldsymbol{X}_{inverse}$ contains variables of such as paired joint angles $q_{knee,left}$ and paired muscle activations e.g. $F_{t,soleus,right}$. $\overline{\boldsymbol{X}}_{inverse}$ contains the same set of state variables as $\boldsymbol{X}_{inverse}$ with the ordering of the paired states swapped in indices. $\boldsymbol{X}_{oppose}$ contains only a number the state variables related to pelvis and lumbar joint such as $q_{pelvos,tz}$, the lateral translation of pelvis.

Equality constraints described in Equation 12, Equation 13 and Equation 14 were modified when relaxing the symmetry assumption:

$$q_{pelvis,tx}(t_f) = t_f v_{target}, \quad (15)$$

$$\boldsymbol{X}_{equal}(t_0) = \boldsymbol{X}_{equal}(t_f), \quad (16)$$

where t_f is the full gait cycle duration, and $\boldsymbol{X}_{equal}$ contains all state variables except $q_{pelvis,tx}$.

Furthermore, all the state variables are bounded with inequality constraints which are derived from the experimental data of healthy walking [Falisse *et al.*, 2019]. However, the typical range of motion of the joints, as reported in the literature [CDC, 2018; Hamilton, 2011], are used as the upper and lower bounds of joint positions $\boldsymbol{q}$ for the SK model. Some bounds are manually set to prevent interpenetration of the MSK model were also adapted for the skeletal model.

Table 1: Optimisation variables

Model	**States:$\boldsymbol{x}(t)$**	**Controls:$\boldsymbol{u}(t)$**
Full body MSK model [Falisse *et al.*, 2019]	Muscle activations : $\boldsymbol{a}$ Tendon forces : $\boldsymbol{F}_t$ Arm activations : $\boldsymbol{a}_{arms}$ Joint positions : $\boldsymbol{q}$ Joint velocities : $\boldsymbol{v}$	Derivatives of $\boldsymbol{a}$: $\boldsymbol{u}_{da}$ Derivatives of $\boldsymbol{F}_t$: $\boldsymbol{u}_{dFt}$ Arm excitations : $\boldsymbol{e}_{arms}$ Derivatives of $\boldsymbol{v}$ (accelerations): : $\boldsymbol{u}_{dv}$
Lower body SK model	Leg activations : $\boldsymbol{a}_{legs}$ Joint positions : $\boldsymbol{q}$ Joint velocities : $\boldsymbol{v}$	Leg excitations : $\boldsymbol{e}_{legs}$ Derivatives of $\boldsymbol{v}$ (accelerations): : $\boldsymbol{u}_{dv}$

Cost functions

The following nominal cost function was identified to predict healthy human walking in [Falisse *et al.*, 2019]:

$$J = \frac{1}{d}\int_0^{t_f} (w_1\|\dot{E}\|_2^2 + w_2\|a\|_2^2 + w_3\|u_{dv,lt}\|_2^2 + w_4\|T_p\|_2^2 + w_5\|e_{arms}\|_2^2),$$

where d is the distance travelled in the forward direction, t_f is the half gait cycle duration, $\dot{E}$ is the metabolic energy rate, a is muscle activity, u_{dv} are the joint accelerations, T_p are the passive torques, e_{arms} are the arm excitations, and w_{1-5} are the corresponding weight factors.

The cost function was adapted for optimisation using the simplified SK model as:

$$J = \frac{1}{d}\int_0^{t_f} (w_1\|e_{legs}\|_2^2 + w_2\|u_{dv,lt}\|_2^2 + w_3\|T_p\|_2^2),$$

where e_{legs} and w_1, are the leg excitations and the corresponding weight factor. The metabolic energy rate and muscle activity terms associated with muscle models, and arm excitation term associated with arm movements were removed. The values of w_2 and w_3 were not modified since the relative importance of those cost terms should be transferable. A heuristic approach was taken to find w_1 which generats simulated gaits closest to experimental data collected.

Initial guesses

The robustness of the optimisation framework to the choice of initial values was tested in [Falisse *et al.*, 2019], we opt to use *data-informed* method which derive initial guesses of joint states and controls($\boldsymbol{q}, \boldsymbol{v}, \boldsymbol{u}_{dv}$) from experimental data. The states and controls of muscles and torque actuators are initialized with constants across time.

4 Data collection and analysis

4.1 Experimental protocol

Experimental gait data was collected from one healthy adult in the biomechanics lab at the University of Melbourne, equipped with the Vicon motion capture system and dual-belt instrumented treadmill. Experiment scheduling and data collection was affected by Covid-19 outbreaks and restrictions. The participant was instructed to walk on a treadmill at a self selected speed, which came to 1.2 ms^{-1}. The participant was first recorded performing their normal preferred gait. Next, to generate asymmetric data, a restrictive cuff was designed and utilised to limit the movement of the participant's left knee joint.

Ten Vicon cameras (Vicon Motion Systems, Oxford, UK) collected 3D motion of a set of 26 retroreflective markers (spherical, 14 mm, B&L Engineering, CA, USA) at 100 Hz. The markers were bilaterally placed in the pelvic area and on lower-limb segments [Robertson *et al.*, 2013], with 20 functional markers and six to differentiate the two legs. Ground reaction forces (GRFs) were collected at 1 kHz and synchronised with marker data in Vicon Nexus 2.8.1.

4.2 Data analysis

The experimental data was preprocessed with OpenSim 4.1 [Delp *et al.*, 2007; Seth *et al.*, 2018]. The kinematic and kinetic parameters of the skeletal model were personalised using the *Scaling* tool of OpenSim. The *Inverse Kinematics* and *Inverse Dynamics* tools were utilised to compute the joint position and torque trajectories respectively.

The simplified 16 DoF SK model was further modified to incorporate the effect of the restrictive cuff. The proximal end of the cuff was assumed to be fixed at the mid point of left femur, while the contact between distal end of cuff and the mid point of shank was modelled using smoothed Hunt-Crossley force.

5 Results

All simulation was performed on 6 core 10th Generation Intel i5 Processors, optimisation problems introduced in [Falisse *et al.*, 2019] was ran on the same hardware for fair comparisons of computational costs. The supplementary videos of the simulates results are available at

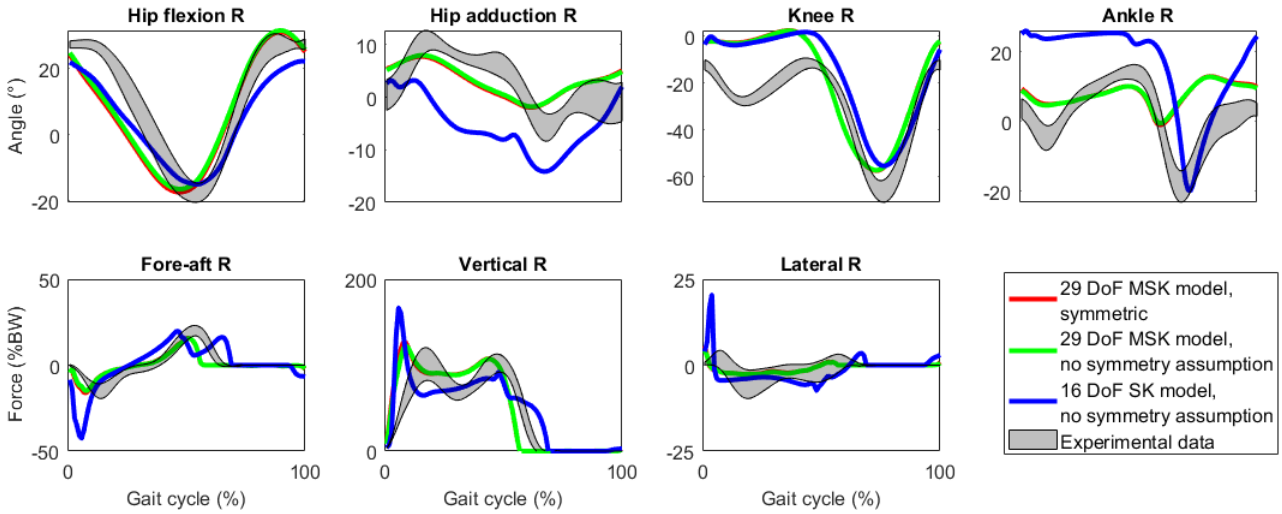

Figure 2: Simulated walking gaits using the MSK and simplified SK biomechanical models and relaxing the symmetry assumption. The joint angles of a selected range of joints are shown in the top row. The ground reaction of the right foot is shown in the bottom row.

the following link: `https://github.com/zhongxiangc/Gait-Simulation-for-Asymmetric-Gait.git`.

5.1 Relaxing symmetry assumption

As introduced in 3.3, the symmetry assumption can be relaxed by changing the equality constraints from Equation 12, Equation 13 and Equation 14 to Equation 15 and Equation 16. Gait patterns were generated by optimising for both half and entire stride using the same MSK model, nominal cost function, and constraints. The optimisation with symmetry assumption took half gait data-informed initial guess, while optimisation without symmetry assumption took full gait initial guess. Additionally, the number of mesh intervals was doubled from 50 to 100 when solving the problem without the symmetry assumption, thus keeping time discretisation between mesh points unchanged. The simulated results were shown in Figure 2 and compared with experimental data collected from [Falisse *et al.*, 2019], because muscle parameters of 29 DoF MSK model were tuned towards the participant in their study. The optimal trajectories found after relaxing the symmetry assumption closely replicate the original solutions. However, the number of variables of the transformed NLP was also doubled, and the problem became much more difficult. Therefore, the computational time increased from 2,552 to 9,646 seconds as shown in Figure 4, which supports the common assumption that optimising for the full stride is more computationally demanding compared to optimising for just one step.

5.2 Reducing model complexity

The simplified 16 DoF skeletal model was used to reduce the high demand in computational resources when optimising for the entire stride. The simulated results using the same data-informed initial guesses and constraints as 5.1 are also shown in Figure 2 and Figure 4 for direct comparison with previous results. The simplified model provides similar estimates for hip and knee flexion, the main difference between the generated gait patterns was the increased dorsiflexion of the ankle joint during the stance phase in the simplified model, which moves the contact sphere to the same line of all leg segments thus reducing the torque experienced by ankle joints. A potential explanation could be that the Achilles tendon resists dorsiflexion of ankle when knee is in the natural position. The anterior muscles of the lower leg are weaker comparing to the posterior ones, and metabolic energy rate and muscle activity costs in the MSK model restricted dorsiflextion of ankle during stance. However, those terms were not present in the SK model since all joints were driven by ideal torque actuators. The push-off phase of gait was shorter which could explain the decrease in stride length. In addition, the hip adduction/abduction had increased to compensate the locking of subtalar joints for weight balance in the lateral direction. The other effect of locking the subtalar joint was that step width increased from 0.08m to 0.26m. And finally, the number of optimisation variables was reduced significantly comparing to the MSK model from 146,500 to 22,642, which lead to the reduction of computational time from 9,646 seconds to 273 seconds.

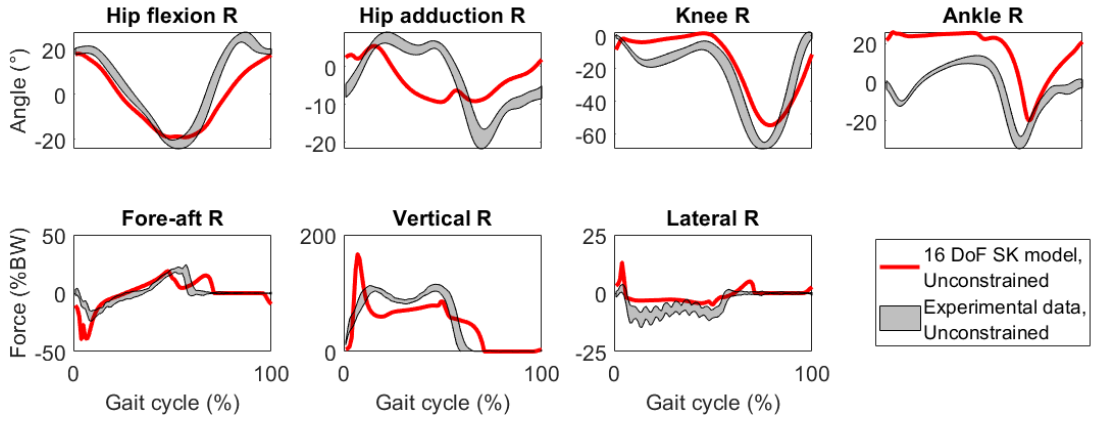

(a) Gait simulation results and experimental data without constraint

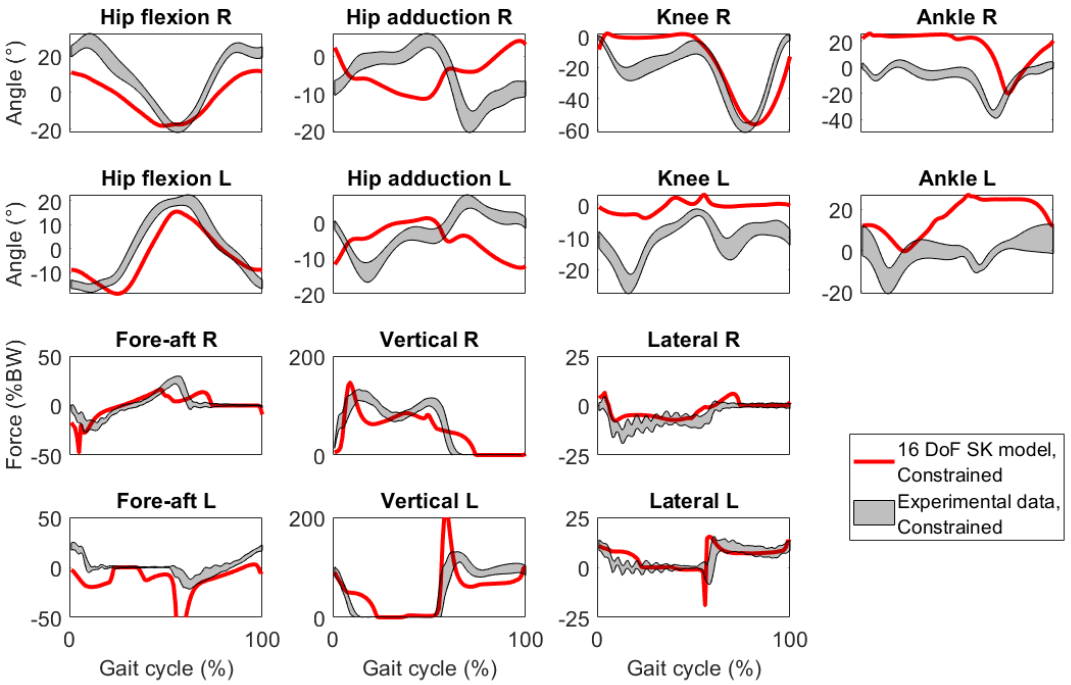

(b) Gait simulation results and experimental data with constrained left knee

Figure 3: Simulated walking gaits using the 16DoF skeletal model with and without left knee constraint. (a) The joint angles of a selected range of joints are shown in the top row. The ground reaction force of the right foot is shown in the bottom row (BW, body weight; GC, gait cycle). The joint angles of the selected joints and ground reaction forces of both sides are shown in (b).

5.3 Add single-sided constraint

For the simplified model, a version which includes the restrictive cuff as described in 4 was also created. In this section, the un-constrained and constrained 16 DoF SK models are scaled with the preliminary data collected. Full gait cycles were simulated using the same cost function and path constraints as 5.2, while joint trajectories of a full gait cycle were used as the initial guesses. The simulated results are shown in Figure 3 and compared with the preliminary data, while the meta-analysis of the simulation are summarised in Figure 4. For both the unconstrained and constrained models, the optimal joint trajectories found were very similar on the right side, the un-constrained side, while the trajectories on the left side were quite different. Comparing to the measured data, the movements of the left knee joint was limited but not

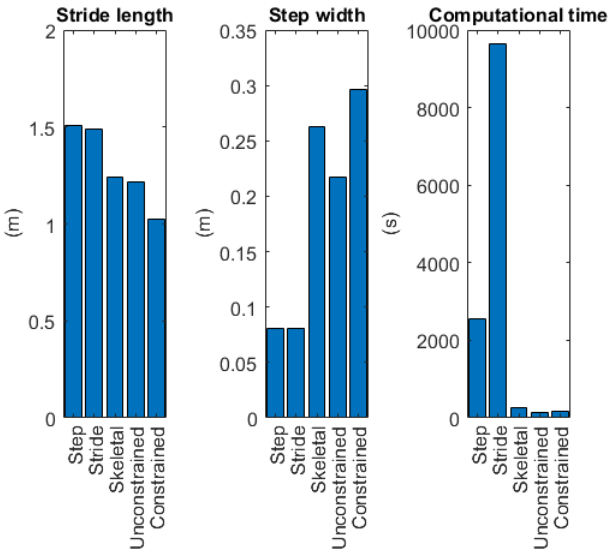

Figure 4: Meta-analysis of gait simulations. The stride length, step width and computational time for simulated results under five conditions are shown. *Step*: 29 DoF MSK model,symmetric; *Stride*: 29 DoF MSK model,no symmetry assumption; *Skeletal*: 16 DoF SK model,no symmetry assumption; *Unconstrained*: 16 DoF SK model, unconstrained; *Constrained*: 16 DoF SK model, constrained.

fully locked, thus the constrained simulation underestimates the movement of the left knee. The movements in hip and ankle joints had to adapt to the restricted knee movements, however, neither of those joints worked harder to compensate the loss of distance travelled. The stride length of the constrained case is 1.03m comparing to the 1.22m in the unconstrained case. The step width of the constrained gait is 0.30 m comparing to 0.22 m of the unconstrained simulation. The computational time for the constrained case is 173 seconds which is 45 seconds or 35% longer than 128 seconds of the unconstrained. This is expected because the initial guesses were generated from the unconstrained trial.

6 Conclusion and future work

Optimal control has been used in this work to simulate both symmetric and asymmetric gaits on various models. The symmetry constraint was relaxed to allow optimisation of the entire stride and permit asymmetric gaits, at the cost of computational resources. Using the skeletal model reduced the computing time by 30 times comparing to the more complex musculoskeletal model. The simulated unconstrained and constrained gait using the personalised skeletal model is close to the experimental data, with the exception of ankle and hip adduction joint trajectories.

Future works will seek to employ techniques such as inverse optimal control to identify the cost function of gait systematically, instead of using heuristic approaches. Another potential direction is to reduce the computational time further to allow real-time applications in the fields of human robot interaction and assistive devices.

Acknowledgment

This work was supported by the Australian Research Council Discovery Grant DP200102402.

References

[Alexander, 1984] R. McN. Alexander. The Gaits of Bipedal and Quadrupedal Animals. *The International Journal of Robotics Research*, 3(2):49–59, June 1984.

[Alexander, 1996] R. McNeill Alexander. *Optima for Animals: Revised Edition*. Princeton University Press, 1996.

[Anderson and Pandy, 2001] Frank C. Anderson and Marcus G. Pandy. Dynamic Optimization of Human Walking. *Journal of Biomechanical Engineering*, 123(5):381–390, May 2001.

[Andersson *et al.*, 2019] Joel A. E. Andersson, Joris Gillis, Greg Horn, James B. Rawlings, and Moritz Diehl. CasADi: a software framework for nonlinear optimization and optimal control. *Mathematical Programming Computation*, 11(1):1–36, March 2019.

[Bataineh *et al.*, 2016] Mohammad Bataineh, Timothy Marler, Karim Abdel-Malek, and Jasbir Arora. Neural network for dynamic human motion prediction. *Expert Systems with Applications*, 48:26–34, April 2016.

[Bazett-Jones *et al.*, 2017] David M. Bazett-Jones, Tyler Tylinksi, Jelena Krstic, Abigail Stromquist, and Jay Sparks. Peak hip muscle torque measurements are influenced by sagittal plane hip position. *International Journal of Sports Physical Therapy*, 12(4):535–542, August 2017.

[CDC, 2018] CDC. Normal joint range of motion study | CDC, December 2018.

[Channon *et al.*, 1992] P. H. Channon, S. H. Hopkins, and D. T. Pham. Derivation of optimal walking motions for a bipedal walking robot. *Robotica*, 10(2):165–172, March 1992.

[Chow and Jacobson, 1971] C. K. Chow and D. H. Jacobson. Studies of human locomotion via optimal programming. *Mathematical Biosciences*, 10(3):239–306, April 1971.

[Chung *et al.*, 2015] Hyun-Joon Chung, Yujiang Xiang, Jasbir S. Arora, and Karim Abdel-Malek.

Optimization-based dynamic 3D human running prediction: effects of foot location and orientation. *Robotica*, 33(2):413–435, February 2015.

[De Groote *et al.*, 2016] Friedl De Groote, Allison L. Kinney, Anil V. Rao, and Benjamin J. Fregly. Evaluation of Direct Collocation Optimal Control Problem Formulations for Solving the Muscle Redundancy Problem. *Annals of Biomedical Engineering*, 44(10):2922–2936, October 2016.

[Delp *et al.*, 2007] Scott L. Delp, Frank C. Anderson, Allison S. Arnold, Peter Loan, Ayman Habib, Chand T. John, Eran Guendelman, and Darryl G. Thelen. OpenSim: Open-Source Software to Create and Analyze Dynamic Simulations of Movement. *IEEE Transactions on Biomedical Engineering*, 54(11):1940–1950, November 2007.

[Ezati *et al.*, 2019] Mahdokht Ezati, Borna Ghannadi, and John McPhee. A review of simulation methods for human movement dynamics with emphasis on gait. *Multibody System Dynamics*, 47(3):265–292, November 2019.

[Falisse *et al.*, 2019] Antoine Falisse, Gil Serrancolí, Christopher L. Dembia, Joris Gillis, Ilse Jonkers, and Friedl De Groote. Rapid predictive simulations with complex musculoskeletal models suggest that diverse healthy and pathological human gaits can emerge from similar control strategies. *Journal of The Royal Society Interface*, 16(157):20190402, August 2019.

[Felis and Mombaur, 2016] Martin L. Felis and Katja Mombaur. Synthesis of full-body 3-D human gait using optimal control methods. In *2016 IEEE International Conference on Robotics and Automation (ICRA)*, pages 1560–1566, May 2016.

[Felis *et al.*, 2015] Martin L. Felis, Katja Mombaur, and Alain Berthoz. An optimal control approach to reconstruct human gait dynamics from kinematic data. In *2015 IEEE-RAS 15th International Conference on Humanoid Robots (Humanoids)*, pages 1044–1051, November 2015.

[Flash and Hogan, 1985] T. Flash and N. Hogan. The coordination of arm movements: an experimentally confirmed mathematical model. *Journal of Neuroscience*, 5(7):1688–1703, July 1985.

[Grimmer and Seyfarth, 2014] Martin Grimmer and André Seyfarth. Mimicking Human-Like Leg Function in Prosthetic Limbs. In Panagiotis Artemiadis, editor, *Neuro-Robotics: From Brain Machine Interfaces to Rehabilitation Robotics*, Trends in Augmentation of Human Performance, pages 105–155. Springer Netherlands, Dordrecht, 2014.

[Hamilton, 2011] Nancy Hamilton. Kinesiology: Scientific basis of human motion. *Faculty Book Gallery*, January 2011.

[Hamner *et al.*, 2010] Samuel R. Hamner, Ajay Seth, and Scott L. Delp. Muscle contributions to propulsion and support during running. *Journal of Biomechanics*, 43(14):2709–2716, October 2010.

[Hull, 1997] David G. Hull. Conversion of Optimal Control Problems into Parameter Optimization Problems. *Journal of Guidance, Control, and Dynamics*, 20(1):57–60, 1997. Publisher: American Institute of Aeronautics and Astronautics _eprint: https://doi.org/10.2514/2.4033.

[Kajita *et al.*, 1992] S. Kajita, T. Yamaura, and A. Kobayashi. Dynamic walking control of a biped robot along a potential energy conserving orbit. *IEEE Transactions on Robotics and Automation*, 8(4):431–438, August 1992.

[Kajita *et al.*, 2001] S. Kajita, O. Matsumoto, and M. Saigo. Real-time 3D walking pattern generation for a biped robot with telescopic legs. In *Proceedings 2001 ICRA. IEEE International Conference on Robotics and Automation (Cat. No.01CH37164)*, volume 3, pages 2299–2306 vol.3, May 2001.

[Kudoh and Komura, 2003] S. Kudoh and T. Komura. C/sup 2/ continuous gait-pattern generation for biped robots. In *Proceedings 2003 IEEE/RSJ International Conference on Intelligent Robots and Systems (IROS 2003) (Cat. No.03CH37453)*, volume 2, pages 1135–1140 vol.2, October 2003.

[Kulić *et al.*, 2016] Dana Kulić, Gentiane Venture, Katsu Yamane, Emel Demircan, Ikuo Mizuuchi, and Katja Mombaur. Anthropomorphic Movement Analysis and Synthesis: A Survey of Methods and Applications. *IEEE Transactions on Robotics*, 32(4):776–795, August 2016. Conference Name: IEEE Transactions on Robotics.

[Kuo, 1995] A.D. Kuo. An optimal control model for analyzing human postural balance. *IEEE Transactions on Biomedical Engineering*, 42(1):87–101, January 1995.

[Lin and Pandy, 2017] Yi-Chung Lin and Marcus G. Pandy. Three-dimensional data-tracking dynamic optimization simulations of human locomotion generated by direct collocation. *Journal of Biomechanics*, 59:1–8, July 2017.

[Lin *et al.*, 2021] Jonathan Feng-Shun Lin, Pamela Carreno-Medrano, Mahsa Parsapour, Maram Sakr, and Dana Kulić. Objective learning from human demonstrations. *Annual Reviews in Control*, 51:111–129, January 2021.

[Meyer *et al.*, 2016] Andrew J. Meyer, Ilan Eskinazi, Jennifer N. Jackson, Anil V. Rao, Carolynn Patten, and Benjamin J. Fregly. Muscle Synergies Facilitate Computational Prediction of Subject-Specific Walking Motions. *Frontiers in Bioengineering and Biotechnology*, 4, October 2016.

[Moraux *et al.*, 2013] Amélie Moraux, Aurélie Canal, Gwenn Ollivier, Isabelle Ledoux, Valérie Doppler, Christine Payan, and Jean-Yves Hogrel. Ankle dorsi- and plantar-flexion torques measured by dynamometry in healthy subjects from 5 to 80 years. *BMC Musculoskeletal Disorders*, 14(1):1–11, December 2013.

[Park and Kim, 1998] J.H. Park and K.D. Kim. Biped robot walking using gravity-compensated inverted pendulum mode and computed torque control. In *Proceedings. 1998 IEEE International Conference on Robotics and Automation (Cat. No.98CH36146)*, volume 4, pages 3528–3533 vol.4, May 1998.

[Rajagopal *et al.*, 2016] Apoorva Rajagopal, Christopher L. Dembia, Matthew S. DeMers, Denny D. Delp, Jennifer L. Hicks, and Scott L. Delp. Full-Body Musculoskeletal Model for Muscle-Driven Simulation of Human Gait. *IEEE Transactions on Biomedical Engineering*, 63(10):2068–2079, October 2016.

[Robertson *et al.*, 2013] D. Gordon E. Robertson, Graham E. Caldwell, Joseph Hamill, Gary Kamen, and Saunders N. Whittlesey. *Research methods in biomechanics 2nd edition*. Human Kinetics, 2013.

[Saidouni and Bessonnet, 2003] Tarik Saidouni and Guy Bessonnet. Generating globally optimised sagittal gait cycles of a biped robot. *Robotica*, 21(2):199–210, March 2003.

[Seth *et al.*, 2018] Ajay Seth, Jennifer L. Hicks, Thomas K. Uchida, Ayman Habib, Christopher L. Dembia, James J. Dunne, Carmichael F. Ong, Matthew S. DeMers, Apoorva Rajagopal, Matthew Millard, Samuel R. Hamner, Edith M. Arnold, Jennifer R. Yong, Shrinidhi K. Lakshmikanth, Michael A. Sherman, Joy P. Ku, and Scott L. Delp. OpenSim: Simulating musculoskeletal dynamics and neuromuscular control to study human and animal movement. *PLoS computational biology*, 14(7):e1006223, July 2018.

[Sherman *et al.*, 2011] Michael A. Sherman, Ajay Seth, and Scott L. Delp. Simbody: multibody dynamics for biomedical research. *Procedia IUTAM*, 2:241–261, January 2011.

[Todorov, 2004] Emanuel Todorov. Optimality principles in sensorimotor control. *Nature Neuroscience*, 7(9):907–915, September 2004. Bandiera_abtest: a Cg_type: Nature Research Journals Number: 9 Primary_atype: Reviews Publisher: Nature Publishing Group.

[Wächter and Biegler, 2006] Andreas Wächter and Lorenz T. Biegler. On the implementation of an interior-point filter line-search algorithm for large-scale nonlinear programming. *Mathematical Programming*, 106(1):25–57, March 2006.

[Xiang *et al.*, 2010] Yujiang Xiang, Hyun-Joon Chung, Joo H. Kim, Rajankumar Bhatt, Salam Rahmatalla, Jingzhou Yang, Timothy Marler, Jasbir S. Arora, and Karim Abdel-Malek. Predictive dynamics: an optimization-based novel approach for human motion simulation. *Structural and Multidisciplinary Optimization*, 41(3):465–479, April 2010.